Radio Frequency Plasma Applications for Space Propulsion

M.D. Carter, F.R. Chang-Díaz, A.V. Ilin†, D.O. Sparks,*
*F.W. Baity Jr., G.C. Barber, R.H. Goulding, E.F. Jaeger, J.P. Squire**

Oak Ridge National Laboratory
Building 9201-2, MS8071, Oak Ridge, TN 37831 (USA)
(*) Advanced Space Propulsion Laboratory, Johnson Space Center, NASA
13000 Space Center Blvd., Houston, TX 77059 (USA)
(†)Lockheed Martin Space Operation Company
13000 Space Center Blvd., Houston, TX 77059 (USA)
Tel. (423)574-1309, Fax (423)576-7926, E-mail cartermd@ornl.gov

Abstract— **Recent developments in solid-state radio frequency (RF) power technologies allow for the practical consideration of RF heated plasmas for space propulsion. These technologies permit the use of any electrical power source, de-couple the power and propellant sources, and allow for the efficient use of both the propellant mass and power. Efficient use of the propellant is obtained by expelling the rocket exhaust at the highest possible velocity, which can be orders of magnitude higher than those achieved in chemical rockets. Handling the hot plasma exhaust requires the use of magnetic nozzles, and the basic physics of ion detachment from the magnetic field is discussed. The plasma can be generated by RF using helicon waves to heat electrons. Further direct heating of the ions helps to reduce the line radiation losses, and the magnetic geometry is tailored to allow ion cyclotron resonance heating. RF field and ion trajectory calculations are presented to give a reasonably self-consistent picture of the ion acceleration process.** [1]

I. Introduction

Radio frequency (RF) power has been successfully used to heat ions in experimental fusion plasmas for several decades [1]. New advances in solid state RF power supplies, as shown in Fig. 1, now permit RF plasma heating techniques to become space relevant (direct to RF power conversion is already $\lesssim 350$ g/kW and decreasing). New high temperature superconductor (HTSC) technologies can also provide the magnetic fields required for both RF application and exhaust nozzle direction. These RF techniques do not use electrodes, scale over a large power range from ~ 100 to $\gtrsim 10^6$ Watts in fusion applications, and will permit the development of rockets with a wide range of specific impulse from 2000 s to > 10000 s. These RF technologies show promise for both earth-orbit transfer (EOT) and for high speed interplanetary applications.

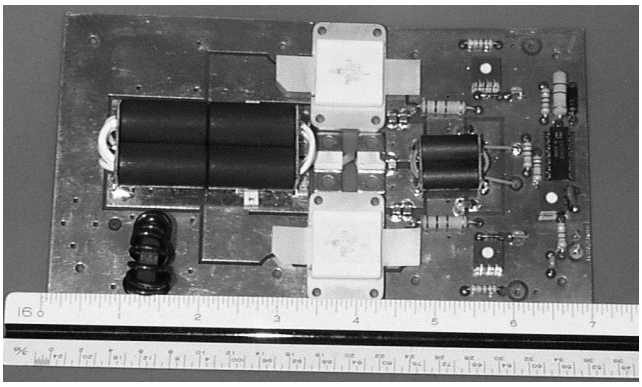

Fig. 1. Solid state amplifiers at 1 KW level now available.

The RF technologies considered here require a magnetic field, both in the ion source region and in the ion acceleration region. The basic way that the RF rocket functions is illustrated in Fig. 2 in terms of the static magnetic field along the rocket axis. A helicon plasma source [2] provides a relatively cold plasma stream with ion energies on the order of $5 - 10$ eV. These ions are then heated in the second section where an ion cyclotron resonance transfers wave energy into ion energy. This energy is initially stored in the ion velocity components perpendicular to the static magnetic field, $E_\perp$, and then converted into directed energy (parallel to the rocket axis) through an adiabatic expansion of the static magnetic field. Eventually, the magnetic field becomes weak and bends away rapidly enough that the adiabatic invariance of the ion's magnetic moment is lost, and the ions escape from the magnetic nozzle. Electrons will escape with the ions because of self-consistent magneto-hydrodynamic currents, cross field (Bohm) diffusion, and other turbulent effects.

The physics of the ion detachment can be estimated by considering the breakdown of the action-angle invariant obtained by averaging over the gyromotion of a

[1]Research sponsored in part by Inter-agency contracts DOE 2044-AA18-Y1 and NASA No. T-7139V.

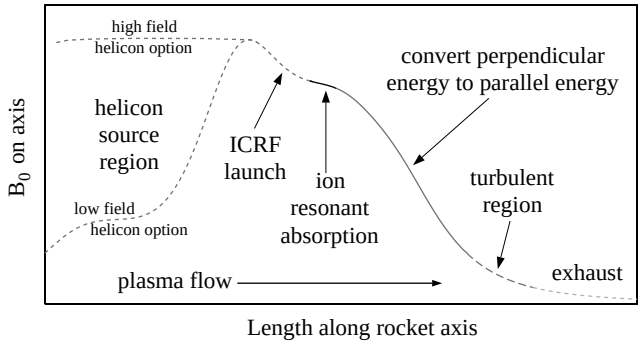

Fig. 2. Magnetic topology of RF heated thruster.

charged particle in a strong magnetic field, $\mu = E_\perp / B_0$ (magnetic moment), where B_0 is the static magnetic field strength. A charged particle's μ is a well conserved quantity until the static magnetic field changes with a scale length comparable to the particle's gyromotion, at which point the orbit effectively becomes unmagnetized.

The action integral used to calculate μ is performed over a gyro-orbit. Therefore, the action invariant (μ) will be destroyed if the orbit becomes very eccentric in a single gyroperiod. Defining ρ to be the average gyro-radius during a gyro-period, and using Δ to denote the change in a quantity after a gyro-period, the orbit becomes unmagnetized when $\Delta\rho \gtrsim \rho$. This relationship can be written as

$$\frac{\Delta\rho}{\rho} = \frac{1}{2}\left[\frac{\Delta\mu}{\mu} - \frac{\Delta\Omega}{\Omega}\right] \approx -\frac{\Delta\Omega}{2\Omega} \gtrsim 1 \qquad (1)$$

where Ω is the gyrofrequency, and the approximation assumes that $\Delta\mu/\mu$ (evaluated at the guiding center location) remains small until the orbit becomes unmagnetized. The quantity $\Delta\Omega/\Omega$ can be estimated using the path of a field line since the exact orbit roughly spirals around a guiding center orbit until μ is no longer conserved. This approximation allows Eq. 1 to be estimated with knowledge of only geometric quantities and the particle's energy. Along a field line $\Delta\Omega/\Omega \approx \Delta s \;\; \hat{b} \cdot \nabla B_0 / |B_0|$ where $\hat{b}$ is a unit vector along the field line, and Δs is the distance traveled along the field line during a gyroperiod. Assuming that most of the particle's energy has been converted into the parallel direction while μ is still conserved, $\Delta s \approx 2\pi v / \langle\Omega\rangle$, where v is the particle's speed and $\langle\Omega\rangle$ is the average gyrofrequency along the orbit. Thus, the estimate for the spatial location where the orbit becomes unmagnetized is given by

$$\left|\frac{\hat{b}\cdot\nabla B_0}{B_0^2}\right| \gtrsim 2200\frac{Z}{\sqrt{AE}} \qquad (2)$$

where A is the atomic weight, Z is the absolute value of the charge state, E is the particle energy in eV, B_0 is in Tesla, and the gradient scale is in m^{-1}.

The required values of B_0 for good ion heating are determined by the ion cyclotron resonance heating (ICRH) process. ICRH requires that the RF frequency, f, match the cyclotron motion of the ion, $f_i = qB_0/(2\pi m) \approx 15ZB_0/A$ (MHz), where, q is the ion charge and m is the ion mass. The coupling of the RF power tends to improve with increasing f, and a minimal RF coupling resistance is needed to efficiently handle the RF power. Preliminary results indicate that $f \gtrsim 1$ MHz will be required for small thruster systems. Only $Z = 1$ is considered to maintain a low energy cost for ion production and easier ion detachment. Thus, $B_0 \gtrsim 0.1$ T is needed for $A = 1$ (Hydrogen); easily obtainable with present HTSC technology. Constraints on HTSC materials may provide a challenge for applying ICRH acceleration techniques to ions with high A.

In section II, we discuss ion propellant choices based on simplified mission requirements. In section III, we discuss RF models used to calculate the RF fields and plasma interactions in RF rocket designs. In section IV, we give our conclusions.

II. Propellant choices

Initial technologies are aimed at low ion mass to ease the magnet and RF design requirements, and thus, have high specific impulse $(I_{sp}) \equiv v/9.8\mathrm{ms}^{-2}$. Although the thrust is reduced for low ion mass, the resulting high I_{sp} can have significant advantages for some applications. First, the high mass propellants are typically rare and expensive noble gases such as Xenon. In addition, maximum practical acceleration energies lead to specific impulse limits for high mass ions such that a large total propellant mass must be launched to reach high final payload speeds. High final payload speeds will be required for practical interplanetary missions, and minimizing the launched propellant mass can lead to lower cost missions or higher delivered payloads.

To demonstrate the advantages of high I_{sp} and low propellant ion mass, consider a simple power balance for a rocket with fixed I_{sp}. The total power into the plasma stream, P_t, is the sum of the power required to produce the plasma stream, P_{ion}, plus the power that provides the kinetic energy (and momentum) for the exhaust. To simplify the ion production model, we define the average energy required to produce an electron/ion pair, E_{ion}, which includes any radiation or other losses incurred when producing the plasma stream. For an ion with atomic weight, A, $P_{ion} \approx 10^8 E_{ion} m'/A$, where P_{ion} is in Watts, E_{ion} is in electron-Volts (eV), and m' is the mass flow rate in kg/sec. In terms of the rocket thrust, $T \equiv m'v$, the exhaust velocity in the rocket frame can be expressed as

$$v = \frac{P_t}{T}\left(1 + \sqrt{1 - \frac{2\times 10^8 E_{ion}}{A\left(P_t/T\right)^2}}\right) \qquad (3)$$

where all units are MKS except for E_{ion} which is in eV. Similarly, the thrust is given by $T = 2AvP_t/(Av^2 + 2\times 10^8 E_{ion})$. From Eq. 3, note that for high ratios of P_t/T, the penalty for ionizing the initial plasma stream becomes negligible. Also note that some schemes for recovering part of the ionization energy may be possible if a low ratio of P_t/T is required.

To define a metric for determining the advantages of various propellants, consider a simplified one-

dimensional mission scenario where an initial mass, M_l, is launched into low earth orbit and is then accelerated by a plasma rocket. We assume that the mission uses a constant exhaust velocity relative to the rocket of v, and expells mass at a constant flow rate, m' until all of the propellant is depleted. The final payload mass, M_p, is then related to the mass initially launched into low earth orbit, M_l, in terms of v and the change in speed of the final payload, ΔV, by

$$M_p = M_l \exp\left(-\Delta V/v\right) \tag{4}$$

The time required to complete the velocity increment of ΔV for the final payload is

$$\Delta t = \frac{M_p}{2P_t}\left(v^2 + 2\times 10^8 E_{ion}/A\right)\left(e^{\Delta V/v} - 1\right) \tag{5}$$

For most missions, it is desirable to maximize the final payload without requiring an excessive amount of time or power to achieve the desired orbit. The ratio of M_l/M_p determines the relative cost to launch the initial payload, and $P_t\Delta t/M_p$ determines an effective time per unit payload mass per unit power. Thus, to simultaneously satisfy both goals, we maximize the quantity $(M_p/M_l)/(P_t\Delta t/M_p)$ with respect to v where P_t and M_p are fixed parameters. We also assume that technology limits the maximum ion energy to be 1000 eV. Of course actual mission calculations are typically much more complicated, and require that the equations be integrated again to obtain the final distances traveled, but the simple results presented here can give a very good indication of the capabilities of the various propellants. Also, note that varying the specific impulse during a mission can result in even better optimization, and the RF technologies can be adjusted during a mission to sustain the optimum performance [3]. These changes could include both variations in the exhaust speed for a single propellant and retuning the system to use different propellants along the trajectory.

High ratios of power to thrust are required to achieve reasonable propellant masses for high final velocities, so the energy required to produce an electron/ion pair becomes negligible compared with the kinetic energy of the exhaust. In Fig. 3(top), the relative initial launch cost for the propellant plus payload is shown as a function of the final payload velocity. The "knee" in each curve is caused by the limit of 1000 eV on the ion energy, and thus the point where I_{sp} can no longer be increased in the optimization process. Delivery time and power can be traded equally in this optimization, and Fig. 3(bottom) shows the product of power and time required to achieve a final payload speed. The light ions have a substantial advantage even for low speed increments, such as EOT, in terms of the total mass that must be initially launched to low earth orbit. The savings in propellant mass can also be traded for higher power sources to help reduce delivery time. Fig. 3(bottom) shows that lighter ion species can also be more efficient in terms of mission time and power when high payload speeds are required, such as for interplanetary missions. Thus, RF methods using light

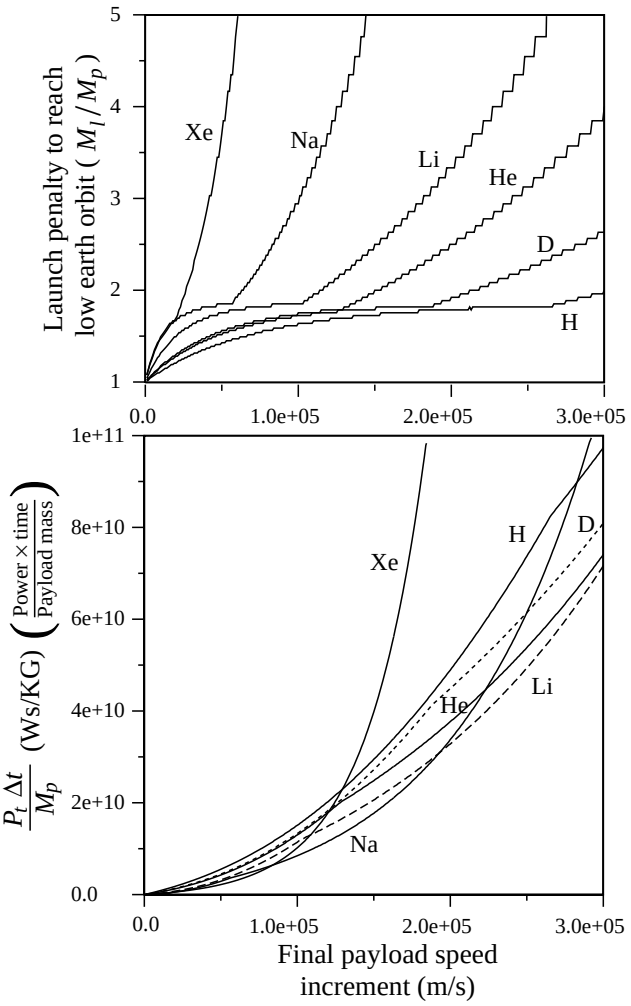

Fig. 3. High I_{sp} gives a big advantage in terms of propellant consumption and final payload speed. Common elements like Li or Na give performance comparable with Xe.

ions could have a substantial impact on future space exploration missions.

III. RF field calculations

Maxwell's equations for a linearized cold plasma response can be written as [1]

$$\nabla \times \vec{E} = i\omega\vec{B} \tag{6}$$

$$\nabla \times \vec{B} = \mu_0\vec{J}_{ext} - i\omega\epsilon_0\mu_0\widetilde{K}\cdot\vec{E} \tag{7}$$

$$\widetilde{K} = \begin{pmatrix} K_\perp & -iK_x & 0 \\ iK_x & K_\perp & 0 \\ 0 & 0 & K_\parallel \end{pmatrix} \tag{8}$$

where

$$K_\perp = 1 - \sum_j \frac{\omega_{pj}^2}{\omega^2 - \Omega_j^2}, \quad K_x = \sum_j \frac{\Omega_j}{\omega}\cdot\frac{\omega_{pj}^2}{\omega^2 - \Omega_j^2},$$

$$K_\parallel = 1 - \sum_j \frac{\omega_{pj}^2}{\omega^2}, \quad \omega_{pj}^2 = \frac{q_j^2 n_j}{\epsilon_0 m_j}, \quad \text{and} \quad \Omega_j = \frac{q_j B_0}{m_j}.$$

In these equations, $\vec{E}$ and $\vec{B}$ are the complex RF electric and magnetic field vectors respectively with implicit

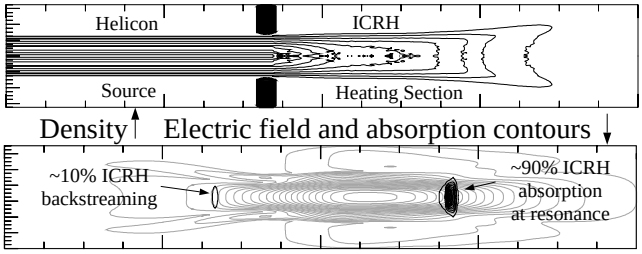

Fig. 4. Converged density and power for EMIR/VASIMR code iteration with contours of electric field having polarization in same direction as ion gyromotion.

$\exp(-i\omega t)$ time dependence, j denotes the electron and ion plasma species, q_j denotes the species charge, m_j denotes the species mass, n_j denotes the species density, B_0 denotes the static magnetic field strength, μ_0 and ϵ_0 are the permeability and permittivity of free space, ω is the driven RF frequency, and $\vec{J}_{ext}$ represents RF current sources from the antenna; all units are MKS. The $\parallel$ and $\perp$ subscripts denote parallel and perpendicular components with respect to the static magnetic field direction, and x denotes the direction orthogonal to both the $\perp$ and $\parallel$ directions.

In the EMIR code [5], cylindrical coordinates are used, and variations in n_j and B are permitted in the axial and radial directions. The RF fields are expanded in a periodic Fourier sum in the azimuthal coordinate to reduce the three-dimensional problem to a weighted sum over two-dimensional solutions. The present version of the code also assumes that $\omega_{pe} >> \omega$ such that the $K_\parallel$ term in the dielectric tensor is very large. This assumption leads to the condition that $E_\parallel$ is very small because of the high mobility of electrons along magnetic field lines, and thus, $E_\parallel = 0$ is assumed. Absorption is introduced in the cold plasma model by adding an imaginary collision frequency to the RF driven frequency, which is equivalent to adding an imaginary particle mass in the dielectric tensor elements.

To obtain a reasonably self-consistent picture of the ICRH absorption, the ion trajectories are followed through the static and RF fields using the VASIMR[6] code. The VASIMR and EMIR codes are then iterated to estimate the ICRH effects on the plasma density. The iteration is performed by calculating the RF fields with the EMIR code, and using these fields to follow nonlinear ion trajectories with the VASIMR code on the gyrofrequency time scale. The ion trajectories are used to generate RF power absorption values and a density input for the next EMIR calculation. The codes are iterated until the density profile becomes reasonably stable, then the collisional absorption parameter in the EMIR code is adjusted and the iteration is continued until the power deposited by the RF system matches the power absorbed by the ion trajectories in a global sense. Results for Helium propellant with 4KW of delivered ICRH power are shown in Fig. 4

An RF powered helicon is presently the leading candidate for the plasma source region shown in Fig. 2. Helicons can be designed to operate over a wide range of magnetic field strengths. Typical values of $B_0 \sim 0.1$ T are used. Generally from the infinite homogeneous dispersion relation, one expects $f \propto B/n_e$ in the limit where $f >> f_{lh}$ where f_{lh} is the lower hybrid frequency[4]. For light elements and high magnetic field strengths, it is also necessary to explore helicon sources in the regime where $f \lesssim f_{lh}$[2]. Other modes of excitation may also be possible[7]. Results from EMIR for the collisional absorption of RF at 13 MHz for the same parameters as shown in Fig. 4 are shown in Fig. 5

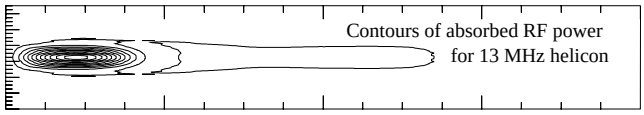

Fig. 5. RF collisional absorption for phased dual half turn antenna in helicon is localized to high density region.

To use a helicon source along with a separate ICRH acceleration section, care must be taken to minimize the ICRH power that can couple back into the source region. If the magnetic field in the source region is greater than that required for ICRH, then little ICRH coupling in the source is possible because there is no location where $f = f_i$. Thus, it is desirable to have the static magnetic field strength in the helicon source greater than that in the ICRH acceleration region. However, other techniques are available to block the ICRH power from the source when the helicon cannot be operated at higher magnetic field strengths than the ICRH section. An example is shown in Fig. 4 where only 10% of the ICRH power flows back into the source region.

IV. Conclusions

High power RF and HTSC technologies now make space applications for RF heated plasma rockets viable. These technologies are easiest to implement for light ions. An electromagnetic code, EMIR, has been coupled with the ion trajectory code, VASIMR, to give reasonably consistent RF field and absorption calculations. Conceptual designs for rockets using these technologies show promise for numerous applications including low cost earth orbit transfers and high speed interplanetary missions.

References

[1] T. H. Stix, "Waves in Plasmas", American Institute of Physics, New York, 1992.

[2] A. R. Ellingboe and R. W. Boswell, "Capacitive, inductive and helicon-wave modes of operation of a helicon plasma source", *Phys. Plasmas*, 1996, Vol. 3, pp 2797-2804.

[3] F. R . Chang-Díaz, et.al., "Research Status of the Variable Specific Impulse Magnetoplasma Rocket", *(Proceedings of Open Systems '98) Transactions of Fusion Technology*, 1999, Vol.35, pp. 87-93.

[4] F. F. Chen, et.al. "Coupled Helicon-Cyclotron Modes: Theory and Experiment", *University of Los Angeles Report LTP-806* June, 1998.

[5] E. F. Jaeger, et.al., "ICRF Wave Propagation and Absorption in Tokamak and Mirror Magnetic Fields", *Computer Physics Comm.*, 1986, Vol.40, pp.33-64.

[6] A. V. Ilin, et.al., "Monte Carlo Particle Dynamicds in a Variable Specific Impulse Magnetoplasma Rocket", *(Proceedings of Open Systems '98) Transactions of Fusion Technology*, 1999, Vol.35, pp. 330-334.

[7] B. N. Breizman, A. V. Arefiev, "Radially Localized Helicon Modes in Nonuniform Plasma", *Institute for Fusion Studies, Univ. of Texas*, Report 871, DE-FG03-96ER-54346-871.